



# AMP-activated protein kinase-dependent autophagy mediated the protective effect of sonic hedgehog pathway on oxygen glucose deprivation-induced injury of cardiomyocytes



Qing Xiao <sup>a, b, 1</sup>, Ya Yang <sup>a, 1</sup>, Yuan Qin <sup>c</sup>, Yan-Hua He <sup>c</sup>, Kui-Xiang Chen <sup>a</sup>, Jian-Wei Zhu <sup>d</sup>, Gui-Ping Zhang <sup>a</sup>, Jian-Dong Luo <sup>a, b, \*</sup>

<sup>a</sup> Department of Pharmacology, Guangzhou Medical University, Guangzhou 510182, PR China

<sup>b</sup> Guangzhou Institute of Cardiovascular Disease, Guangzhou Key Laboratory of Cardiovascular Disease, The Second Affiliated Hospital, Guangzhou Medical University, Guangzhou 510260, PR China

<sup>c</sup> Guangzhou Research Institute of Snake Venom, Guangzhou Medical University, Guangzhou 510182, PR China

<sup>d</sup> Department of Orthopedics, Guangzhou First Municipal People's Hospital Affiliated to Guangzhou Medical University, Guangzhou 510182, PR China

## ARTICLE INFO

### Article history:

Received 3 January 2015

Available online 10 January 2015

### Keywords:

Sonic hedgehog pathway

Autophagy

Cardiomyocytes

Oxygen glucose deprivation

## ABSTRACT

Sonic hedgehog (Shh) pathway has been reported to protect cardiomyocytes in myocardial infarction (MI), but the underlying mechanism is not clear. Here, we provide evidence that Shh pathway induces cardiomyocytes survival through AMP-activated protein kinase-dependent autophagy. Shh pathway agonist SAG increased the expression of LC3-II, and induced the formation of autophagosomes in cultured H9c2 cardiomyocytes under oxygen glucose deprivation (OGD) 1 h and 4 h. Moreover, SAG induced a profound AMP-activated protein kinase (AMPK) activation, and then directly phosphorylated and activated the downstream autophagy initiator Ulk1, independent of the autophagy suppressor mammalian target of rapamycin (mTOR) complex 1. Taken together, our results have shown that Shh activates AMPK-dependent autophagy in cardiomyocytes under OGD, suggesting a role of autophagy in Shh-induced cellular protection.

© 2015 Elsevier Inc. All rights reserved.

## 1. Introduction

Sonic hedgehog (Shh) plays a critical role in several tissues during embryonic and postnatal development and adult life [1–9]. Shh signaling occurs through the interaction of the Shh protein with its receptor, Ptc1, and then removes the inhibition of the smoothened receptor. This leads to the activation of a transcription factor, Gli, which induces the expression of downstream target genes, including Ptc1 and Gli1 [10–12].

More evidence reveals that Shh pathway is tightly related to cardiovascular disease. Recent reports from our and others' labs demonstrated that Shh pathway was upregulated in both acute and chronic MI [8,13], and the cardiomyocytes (CMs) were preserved after activation of Shh pathway [8,14,15]. In the absence of Shh

signaling, loss of coronary blood vessels led to tissue hypoxia, cardiomyocyte cell death, heart failure, and subsequent lethality [16]. However, it remains unknown how Shh regulates CMs survival.

Autophagy is an intracellular degradation process of long lived proteins and excess or dysfunctional organelles that can be identified by electron microscopy [17]. During autophagy, the cytosolic form of microtubule-associated protein 1 light chain 3–1 (LC3-I) is converted to the phosphatidylethanolamine-conjugated form of LC3 (LC3-II) to promote autophagosome formation [18]. Therefore, the increase of expression of LC3-II has been widely used to indicate activation of autophagy [19].

Autophagy, which promotes cell survival, occurs in myocardial infarction (MI), it plays a protective role in MI-induced death of CMs [20,21]. Both Shh pathway and autophagy are important for CMs survival, but it remains unknown whether Shh pathway stimulates autophagy of CMs. Therefore, the current study was designed to examine whether Shh pathway protects against oxygen glucose deprivation-induced injury of CMs through autophagy. Our results demonstrate that: 1) Shh pathway stimulated autophagy in H9c2 cardiomyocytes under oxygen glucose

\* Corresponding author. Department of Pharmacology, Guangzhou Medical University, Guangzhou 510182, China. Fax: +86 20 8134 0137.

E-mail address: [jia dongluo@hotmail.com](mailto:jia dongluo@hotmail.com) (J.-D. Luo).

<sup>1</sup> These authors contributed equally to this work.

deprivation (OGD). 2) Autophagy inhibition impaired Shh pathway-induced cell survival and apoptosis inhibition of H9C2 cardiomyocytes under OGD. 3) Shh pathway-induced autophagy involves activation of AMPK.

## 2. Methods

### 2.1. Reagents

The rat cardiomyocyte cell line H9C2 was purchased from American Type Culture Collection (ATCC CRL-1446); DMEM, trypsin, and fetal bovine serum were purchased from Invitrogen, USA; cell culture plates were purchased from Corning Inc., USA. MTT (3-(4,5)-dimethylthiazoliazol (-z-y1)-3,5-di-phenyltetrazolium bromide) were purchased from KeyGEN, China. TUNEL assay kit was purchased from Roche. Rabbit anti-Ptc1 antibody, anti-LC3 antibody, anti-GAPDH antibody and anti-ULK1 antibody kit were respectively purchased from Millipore, Abcam, Sigma, Cell Signal and Santa Cruz. Goat anti-Gli1 antibody was purchased from R&D. SAG1.3, 3-MA and compound C were purchased from Merck. The secondary antibodies (HRP-conjugated affinity purified goat anti-rabbit IgG and HRP-conjugated affinity purified rabbit anti-goat IgG) were purchased from Santa Cruz.

### 2.2. Cell culture and treatments

The H9C2 cell line, a subclone of the original clonal cell line, was derived from embryonic rat heart tissue. The cells were cultured in DMEM medium (25 mM glucose) supplemented with 10% FBS at 37 °C under an atmosphere of 5% CO<sub>2</sub> and 95% air. Briefly, cells were reseeded in the appropriate plate with culture medium containing 10% FBS for 24 h. Cells were then serum-starved for 12 h, followed by drug treatment in 2% FBS for 12 h, and then stimulated by OGD 1 h or 4 h.

### 2.3. Oxygen glucose deprivation (OGD)

After the cells had adhered, the cell culture medium was replaced with serum-free and glucose-free DMEM, and the cells were then placed in a 37 °C incubator at 5% CO<sub>2</sub>, 1% O<sub>2</sub>, and 94% N<sub>2</sub>.

### 2.4. MTT assay

Cell survival was measured using MTT assay (12, 30). At the end of treatment, cells were incubated with MTT reagent (KeyGEN, China) for 4 h, followed by measurement of absorbance at 570 nm using a spectrophotometer.

### 2.5. Tunnel assay

H9C2 cells were evenly plated into 48-well plates, with 0.5 ml of a  $5 \times 10^4$  cells/ml solution placed in each well. After treatment, fix air dried cell samples with a freshly prepared 4% paraformaldehyde for 1 h at 15–25 °C, rinse plates with PBS, incubate in permeabilisation solution (0.1% Triton X-100 in 0.1% sodium citrate) for 2 min on ice, rinse plates twice with PBS, dry area around sample, add 50 µl TUNEL reaction mixture (Roche) on sample, and then incubate slide in a humidified atmosphere for 60 min at 37 °C in the dark, rinse plates with PBS for 3 times. After that, DAPI was added to stain the nucleus for 10 min at room temperature. The plates were respectively stimulated by 540 nm and 350 nm.

### 2.6. Flow cytometry detecting FITC-Annexin V positive apoptotic cells

Cell apoptosis was detected by the Annexin V Apoptosis Detection Kit (BD, USA) according to the manufacturer's protocol. Briefly, cells with indicated treatment were stained with FITC-Annexin V and propidium iodide (PI). Both early (Annexin V+/PI-) and late (Annexin V+/PI+) apoptotic cells were sorted by fluorescence-activated cell sorting (FACS) (Beckman Coulter, Inc., Brea, CA). Cell apoptosis was reflected Annexin V percentage.

### 2.7. MDC staining

Autophagosomes in the cells were detected with monodansylcadaverine (MDC) staining using the method as previously described (5). Briefly, the cells were incubated with 0.05 mM MDC (Sigma) in Hanks' buffered salt solution at 37 °C for 10 min. After being washed three times with 0.1 M PBS, MDC-labeled autophagosomes were examined with a confocal laser scanning microscope. The cells containing MDC-labeled autophagosomes were counted in  $\times 200$  fields (five sequential fields were counted and averaged per coverslip) for three coverslips in each experiment as a percentage of total cell number.

### 2.8. Western blot analysis

Western blot analysis was performed for Shh pathway and LC3 as described [8,15,22,23]. Briefly, equal amounts of protein (30 mg) were separated on SDS–polyacrylamide gels (10% or 15%) and electrotransferred to polyvinylidene difluoride membranes (Millipore). The membranes were incubated with Ptc1 (1:1000 dilution, Abcam), Gli1 (1:1000 dilution, R&D systems), LC3 (1:1000 dilution, Sigma) or GAPDH (1:1000 dilution; Santa Cruz Biotechnology), and incubated with either goat anti-rabbit or rabbit anti-mouse second antibody (1:5000 dilution; Santa Cruz Biotechnology) for 1 h at room temperature. Blots were developed using a supersignal west pico chemiluminescent substrate (Pierce Manufacturing), and molecular band intensity was determined by densitometry (Bio-Rad image software).

### 2.9. Co-immunoprecipitation (Co-IP)

Cell lysates (1000 µg) in 1 ml lysis buffer containing 1% Triton and 0.3% CHAPS were pre-cleared with 30 µl of protein SAG Activates AMPK-Dependent Autophagy IgA/G-beads (Santa Cruz) for 30 min at 4 °C. After centrifugation for 10 min at 4 °C in a micro-centrifuge, the supernatant was rotated overnight with 2 µg of indicated primary antibody (anti-AMPK $\alpha$ 1/2, Santa Cruz). Protein IgA/G-beads (35 µl) were added to the supernatants for 2 h at 4 °C. Then the pellets were washed six times with lysis buffer, resuspended in lysis buffer, and then assayed in western-blots to detect phospho- and total-Ulk1 and AMPK $\alpha$ .

### 2.10. Statistical analysis

All data were analyzed with the statistical software GraphPad Prism 5.0, and all values are expressed as means  $\pm$  SEM. The differences between two groups were analyzed using Student's unpaired t-test, and differences between three or more groups were evaluated via one-way ANOVA with Bonferroni correction. A probability value of  $\leq 0.05$  was considered significant.

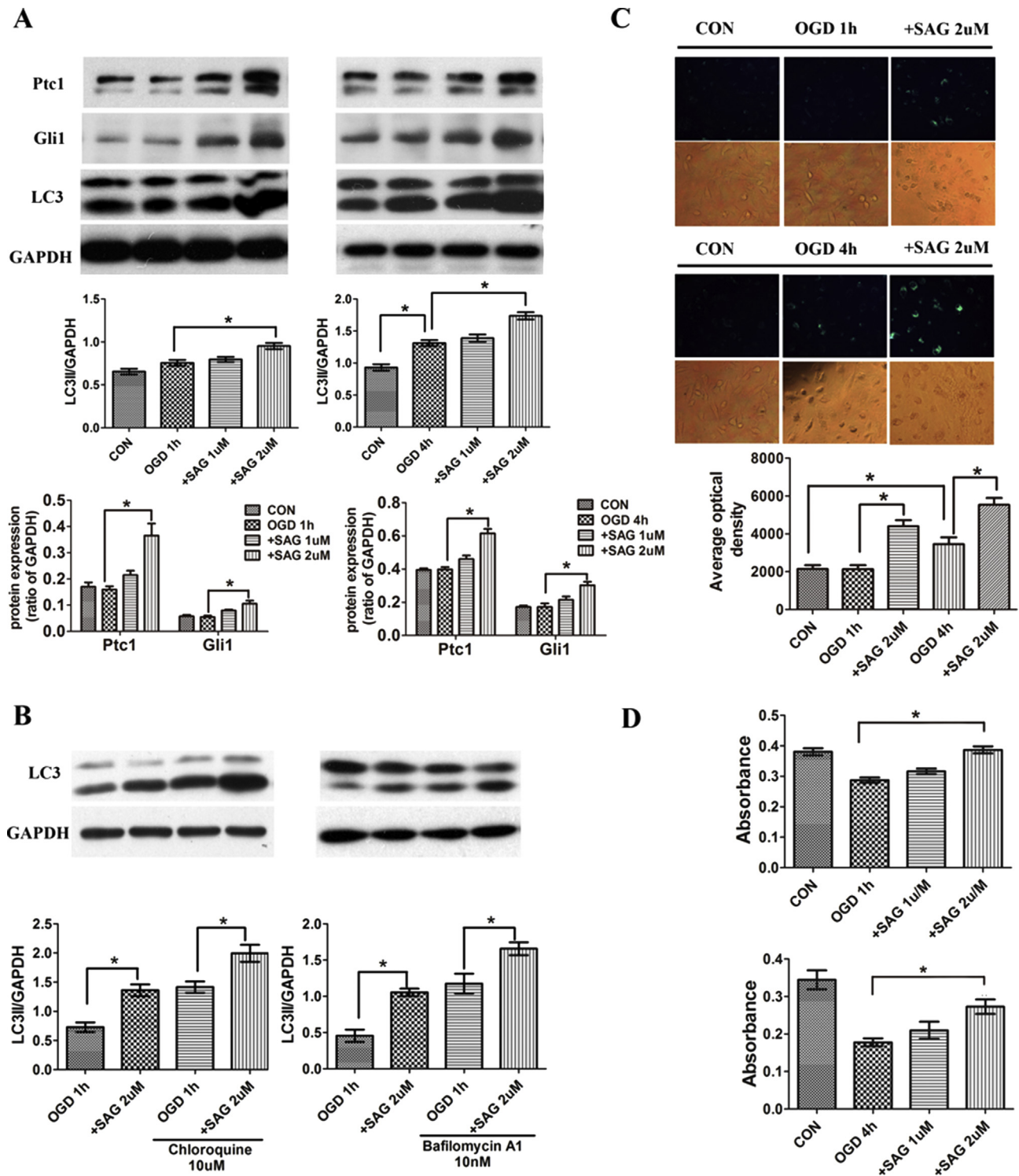


**Fig. 1.** Shh pathway induces autophagy in H9c2 cardiomyocytes under OGD. Cultured H9c2 cardiomyocytes were treated with SAG (1, 2  $\mu$ M) 12 h before OGD 1, 4 h, Ptc1, Gli1, LC3 were detected by western blots as described (A); the average optical density of autophagosomes was recorded (400 $\times$ ) (B). Cultured H9c2 cardiomyocytes were treated with SAG (2  $\mu$ M) plus lysosomal protease inhibitors chloroquine (10  $\mu$ M) or autophagosome-lysosome fusion inhibitor bafilomycin A1 (10 nM) 12 h before OGD 1 h, LC3 were detected by western blots as described (C) Cell viability was analyzed by MTT assay (D).

### 3. Results

#### 3.1. Shh pathway stimulated autophagy in H9C2 cardiomyocytes under OGD

The aim of this current study was to investigate the potential role of autophagy in the protection of Shh pathway in cardiomyocytes under OGD, and to elaborate the underlying mechanisms. Firstly, the potency of Shh pathway agonist SAG should be verified. Administration of Shh pathway agonist SAG (2  $\mu$ M) 12 h before OGD significantly induced the Shh pathway, which was confirmed by the upregulated protein level of Ptc1 and Gli1 (Fig. 1A), and protected the injured H9C2 cells (Fig. 1D) under OGD. Then, the autophagy flux in the activation of Shh pathway was examined. SAG (2  $\mu$ M) increased the expression of LC3-II in H9C2 cardiomyocytes under OGD 1 h (Fig. 1A). When OGD continued to 4 h, the endogenous autophagy was activated, and SAG led to a further enhancement in LC3-II expression (Fig. 1A). Besides, autophagosomes were also detected here, and the result showed that SAG significantly increased the autophagosomes in OGD 1 h and OGD 4 h respectively compared to no drug treatment (Fig. 1C).

It is well known that LC3-II itself will be degraded in autolysosomes during autophagy [24]. Therefore, treatment with lysosomal protease inhibitors chloroquine or autophagosome-lysosome fusion inhibitor bafilomycin A1 will enhance the level of LC3-II if Shh indeed increases autophagy flux. As expected, pretreatment with bafilomycin A1 (10 nM) or chloroquine (10  $\mu$ M) in SAG group for 12 h led to a further promotion in the expression of LC3-II (Fig. 1B). These results suggested that Shh pathway promoted the survival of H9C2 cardiomyocytes in OGD, which was accompanied by the activation of autophagy pathway.

#### 3.2. Autophagy inhibition impaired Shh pathway-induced survival of H9C2 cardiomyocytes under OGD

To test the potential role of autophagy in Shh pathway-induced cardiomyocytes survival in OGD, firstly we used 3-MA as a potent autophagy inhibitor to interrupt Shh induced-autophagy. Western blot results showed that elevated level of LC3-II due to treatment with SAG was significantly declined by treatment with 3-MA in OGD 1 h or OGD 4 h (Fig. 2A). Fluorescence analysis showed similar results that autophagosomes were both decreased in OGD 1 h and OGD 4 h after pretreatment with 3-MA in SAG group (Fig. 2B). Importantly, MTT assay showed that pretreatment with 3-MA 12 h before OGD 1 h or OGD 4 h significantly decreased Shh pathway-induced cell survival (Fig. 2C). These results suggested that autophagy mediated Shh pathway-induced survival of cardiomyocytes under OGD.

#### 3.3. Autophagy inhibition weakened Shh pathway induced-apoptosis inhibition of H9C2 cardiomyocytes under OGD

While sustained and rigorous autophagy promotes cell apoptosis, mild or moderate autophagy is cell protective [25–27]. Above results have shown that autophagy inhibition by 3-MA impaired Shh pathway-induced cell survival in OGD (Fig. 2), we then tested if this was due to enhanced cell apoptosis. Firstly, our results presented a significant apoptosis in OGD 4 h rather than OGD 1 h (Fig. 3). As shown in Fig. 3A, the autophagy inhibitor 3-MA brought about more Tunnel positive cells compared to SAG group in OGD 4 h. Moreover, flow cytometry showed that 3-MA significantly interfered Shh pathway induced-apoptosis inhibition in OGD 4 h (Fig. 3B). These results suggested that autophagy inhibition weakened the decrease of Shh pathway in apoptosis of cardiomyocytes under OGD.

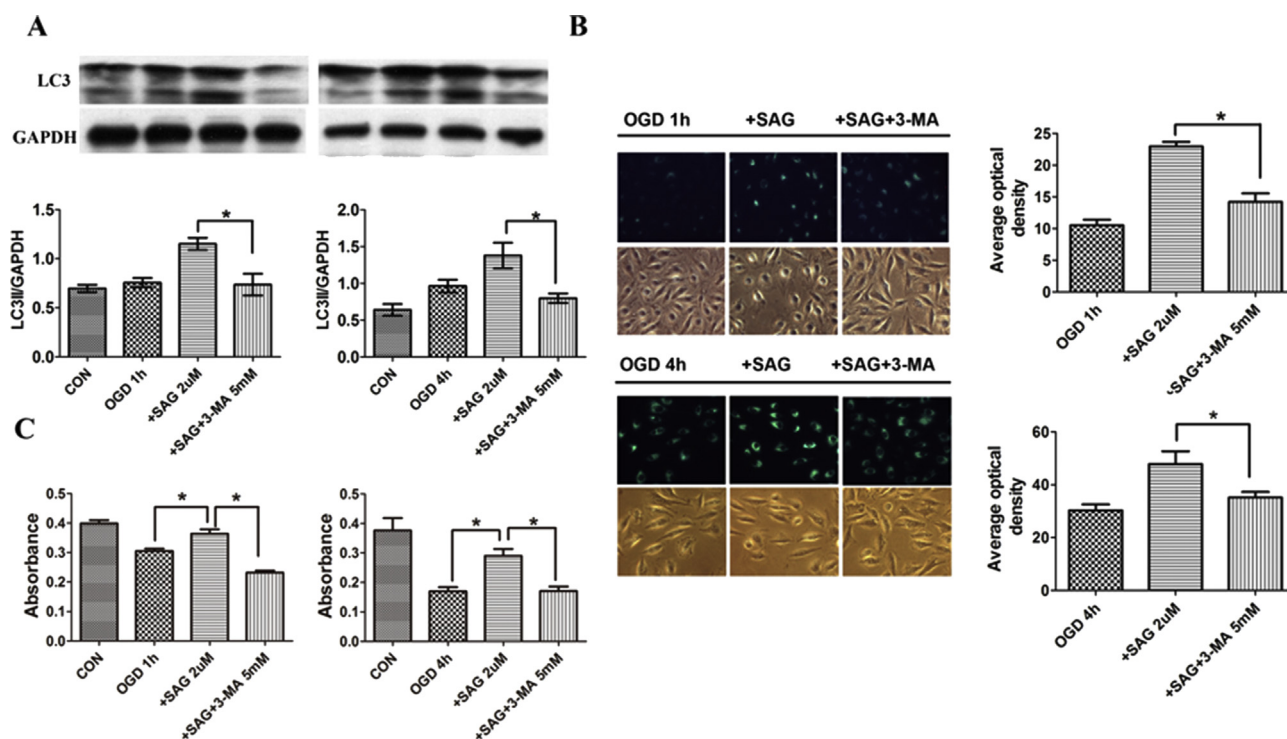
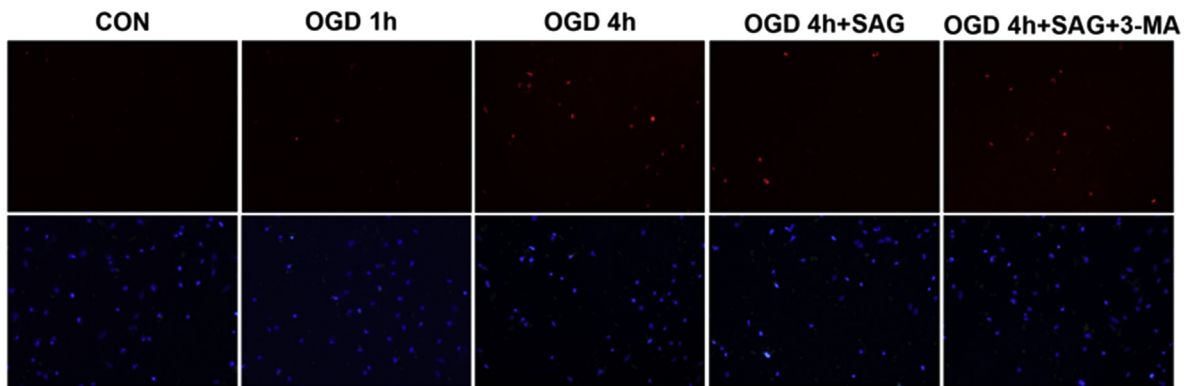


**Fig. 2.** Autophagy inhibition impaired Shh pathway-induced survival of H9C2 cardiomyocytes under OGD. Cultured H9C2 cardiomyocytes were treated with SAG (2  $\mu$ M) plus 3-MA (5 mM) 12 h before OGD 1, 4 h, LC3 were detected by western blots as described (A); the average optical density of autophagosomes was recorded (400 $\times$ ) (B); cell viability was analyzed by MTT assay (C).

A



B

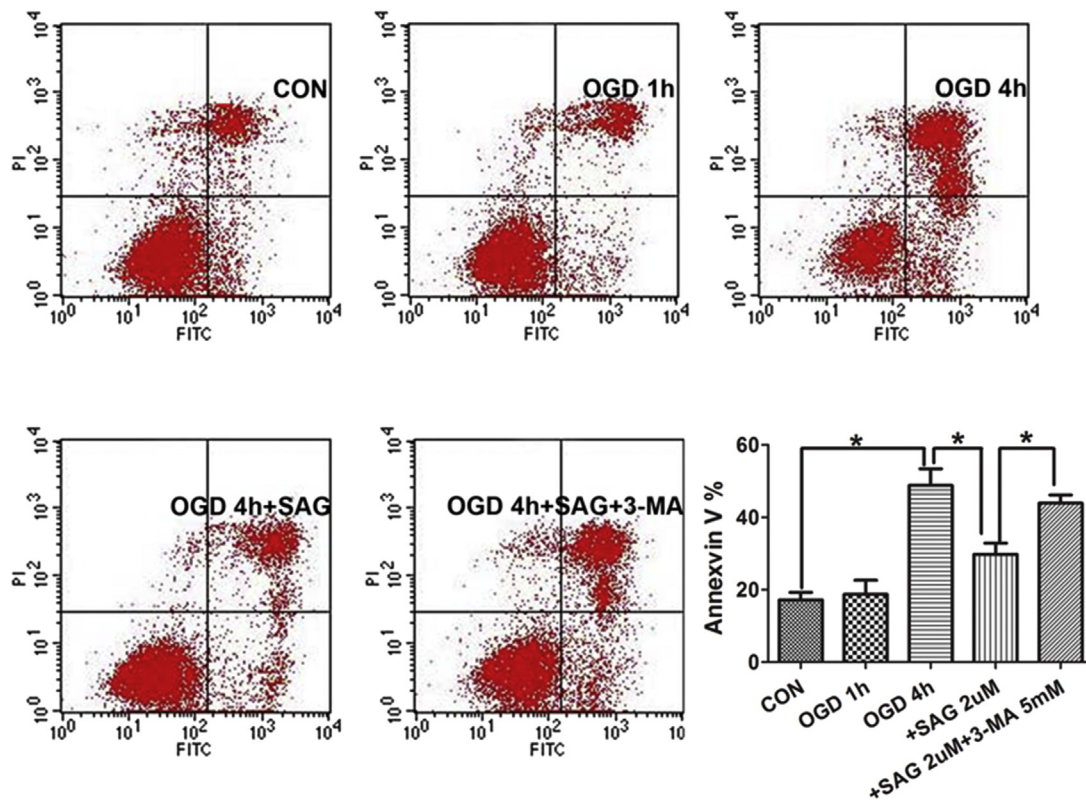


**Fig. 3.** Autophagy inhibition weakened Shh pathway induced-apoptosis inhibition of H9C2 cardiomyocytes under OGD. Cultured H9C2 cardiomyocytes were treated with SAG (2  $\mu$ M) plus 3-MA (5 mM) 12 h before OGD 1, 4 h, apoptotic cells were detected by TUNEL assay (200 $\times$ ) (A), Annexin V positive cells were sorted by FACS (B).

### 3.4. Shh pathway-induced autophagy involves activation of AMPK

Next we focused on the underlying mechanism of autophagy induction by Shh pathway. As discussed, activation of AMPK is important for autophagy induction [28,29]. We first examined AMPK activation in SAG-treated cardiomyocytes. AMPK activation was reflected by AMPK $\alpha$ 1 phosphorylation at Thr 172. As demonstrated, a profound AMPK activation was observed in OGD 1 h after SAG treatment, confirmed by the phosphorylation of AMPK $\alpha$ 1 (Fig. 4A). As we know, activation of AMPK induces autophagy through at least two following mechanisms [28,30]: 1. By directly phosphorylating and activating of Ulk1, the autophagy initiator; 2.

By inhibiting the mammalian target of rapamycin (mTOR) complex 1 (mTORC1), the autophagy suppressor. Our western blot analysis showed that SAG induced autophagy activation domain Ulk1<sup>555</sup> phosphorylation but have no significance in the phosphorylation of mTOR partner Raptor and mTOR downstream p70 S6K, and also its downstream autophagy inhibition domain Ulk1<sup>757</sup> (Fig. 4A). Co-IP results in Fig. 4A further confirmed that Shh pathway induced AMPK/Ulk1 association in cardiomyocytes, which appeared to simultaneously cause Ulk1<sup>555</sup> and AMPK phosphorylation. All above results suggested that Shh pathway indeed activated the autophagy pathway upstream AMPK and through direct AMPK/Ulk1 association to phosphorylate the downstream Ulk1.

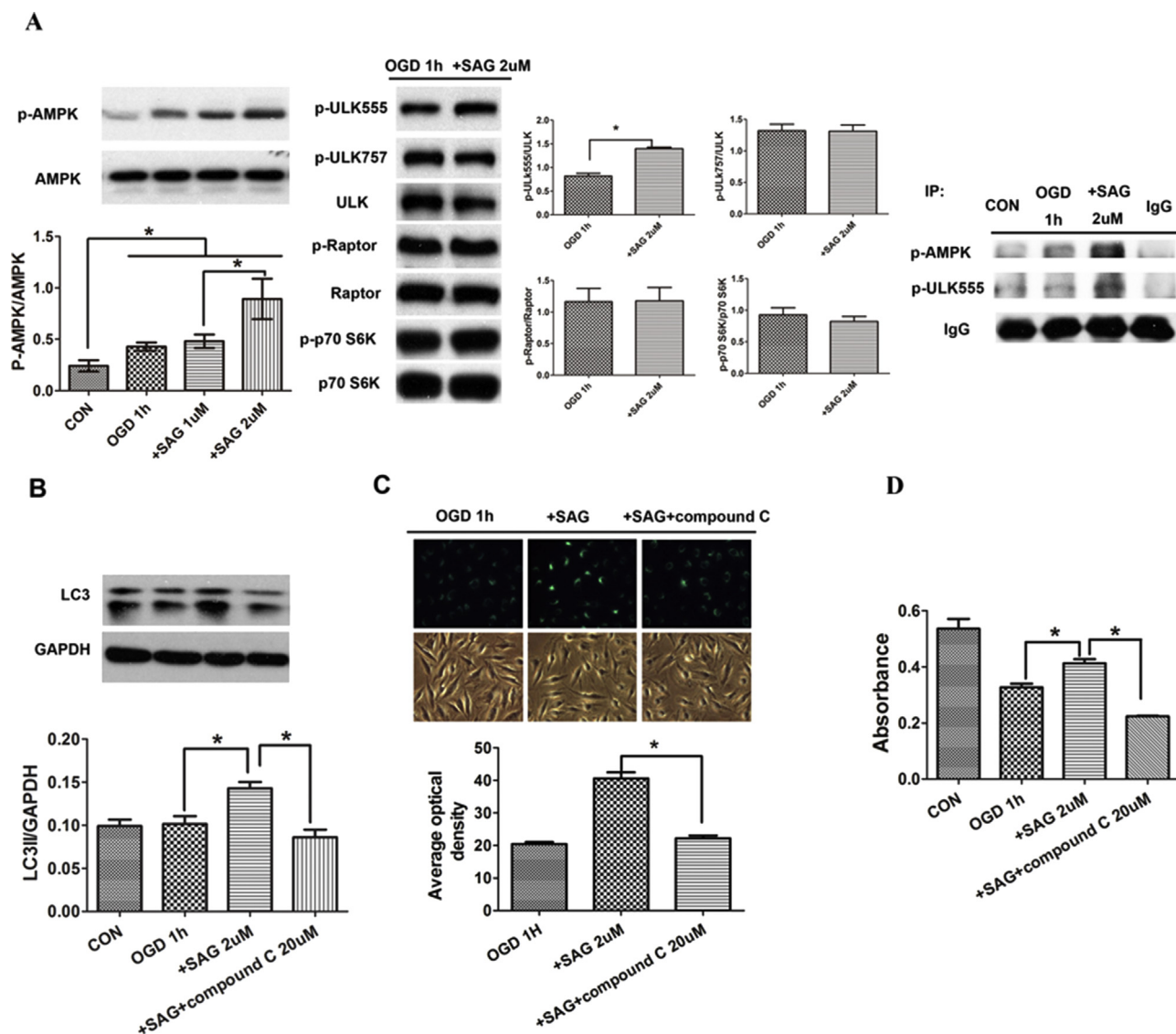


**Fig. 4.** Shh pathway-induced autophagy involves activation of AMPK. Cultured H9c2 cardiomyocytes were treated with SAG (1, 2  $\mu$ M) 12 h before OGD 1 h, p-AMPK/AMPK and downstream p-Raptor/Raptor, p-p70S6K/p70S6K, p-ULK1<sup>555</sup> or ULK1<sup>757</sup>/ULK1 were detected by western blots as described; the association between AMPK $\alpha$  (total and p-) and ULK1 (total and p-) were examined by co-IP (A). Cultured H9c2 cardiomyocytes were treated with SAG (2  $\mu$ M) plus compound C (20  $\mu$ M) 12 h before OGD 1 h, LC3 were detected by western blots as described (B); the average optical density of autophagosomes was recorded (400 $\times$ ) (C); cell viability was analyzed by MTT assay (D).

On the other hand, AMPK inhibitor Compound C significantly inhibited Shh pathway-induced LC3-II expression (Fig. 4B) and autophagosomes in cardiomyocytes (Fig. 4C), correspondingly, cardiomyocytes viability loss were increased in OGD 1 h (Fig. 4D). All these results indicated that activation of AMPK by Shh pathway mediates autophagy in cardiomyocytes.

#### 4. Discussion

Here we observed that Shh pathway induced autophagy in cultured cardiomyocytes in OGD. Inhibition of autophagy by its inhibitor 3-MA, disturbed Shh pathway-induced cell viability and apoptosis inhibition in OGD, indicating that autophagy induction by Shh pathway was against cell death and apoptosis. For the mechanism study, we proposed that AMPK activation by Shh pathway mediated autophagy activation. AMPK inhibition by compound C suppressed Shh pathway-induced autophagy in cardiomyocytes, thus reducing cell viability.

It has been shown by other laboratory that Shh pathway activates autophagy in vascular smooth cells. The relationship of Shh pathway and autophagy in cardiomyocytes and the underlying mechanisms, however, are not fully understood.

Here, we discovered that Shh pathway induced autophagy in cardiomyocytes under OGD, and the autophagy mediated the protective effect of Shh pathway to cardiomyocytes injury by OGD. Moreover, we discovered that Shh pathway induced significant AMPK activation in cultured cardiomyocytes, which promoted Ulk1 activation and autophagy initiation. Kim et al., has demonstrated a molecular mechanism for regulation of Ulk1, the autophagy trigger, by AMPK. AMPK activates autophagy by directly binding and activating Ulk1 through phosphorylation of Ser 555. Following studies have identified other possible phosphorylation sites of Ulk1 by AMPK [31,32]. Reversely, autophagy is inhibited by the mammalian target of rapamycin (mTOR). mTOR phosphorylates Ulk1 at Ser 757 to lock Ulk1 into its complex, and stops Ulk1 from binding to AMPK [28,32]. In the current study, we found that Shh pathway had no

effect on mTOR pathway including its partner Raptor, its downstream molecular p70 S6K and autophagy inhibition domain Ulk1<sup>757</sup>, but notably activated AMPK directly associated and phosphorylated Ulk1 at Ser 555, so it might be the key mechanism for autophagy induction. This proposal was further supported by the fact that compound C abolished Shh pathway-induced autophagy.

AMPK activation dictates energy metabolism, gene transcription, cell mitosis and autophagy through regulating its many downstream kinases [31,33]. However, the definitive role of AMPK in cell survival or death is still controversial. A number studies have found that sustained AMPK activation under severe stress conditions may inhibit cell growth and promote cancer cell death [34–36]. Others found that AMPK is pro-survival [37,38]. One explanation is that, depends on intensity of the stress, AMPK might coordinate with other kinases to rescue cells when facing minor or moderate stresses, or to promote cell death when the rescue fails. In our system, we observed that AMPK activation by Shh pathway was anti-cell death, while AMPK inhibition prevented cardiomyocytes survival by Shh pathway in cardiomyocytes under OGD.

In conclusion, we here found that Shh pathway induces autophagy in cardiomyocytes through AMPK activation, which serves as a negative regulator against cell apoptosis and death under OGD. AMPK-dependent autophagy might represent a novel mechanism for Shh pathway activation in the therapy of ischemic heart disease.

### Conflict of interest

None.

### Acknowledgments

This work was supported by the National Natural Science Foundation of China (No. 81173062 to Dr. JD Luo and No. 81302767 to Dr. Qing Xiao), and Science and Information Technology of Guangzhou (No.12C22021631 to Dr. JD Luo).

### References

- [1] R.D. Paladini, J. Saleh, C. Qian, G.X. Xu, L.L. Rubin, Modulation of hair growth with small molecule agonists of the hedgehog signaling pathway, *J. Invest. Dermatol.* 125 (4) (2005 Oct) 638–646.
- [2] A.P. McMahon, P.W. Ingham, C.J. Tabin, Developmental roles and clinical significance of hedgehog signaling, *Curr. Top. Dev. Biol.* 53 (2003) 1–114.
- [3] C.M. Nielsen, J. Williams, G.R. van den Brink, G.Y. Lauwers, D.J. Roberts, Hh pathway expression in human gut tissues and in inflammatory gut diseases, *Lab. Invest.* 84 (12) (2004 Dec) 1631–1642.
- [4] Y. Katoh, M. Katoh, Hedgehog signaling pathway and gastrointestinal stem cell signaling network (review), *Int. J. Mol. Med.* 18 (6) (2006 Dec) 1019–1023.
- [5] J.K. Sicklick, Y.X. Li, A. Melhem, E. Schmelzer, M. Zdanowicz, J. Huang, et al., Hedgehog signaling maintains resident hepatic progenitors throughout life, *Am. J. Physiol. Gastrointest. Liver Physiol.* 290 (5) (2006 May) G859–G870.
- [6] C. Vaillant, D. Monard, SHH pathway and cerebellar development, *Cerebellum* 8 (3) (2009 Sep) 291–301.
- [7] R. Pola, L.E. Ling, M. Silver, M.J. Corbley, M. Kearney, R. Blake Pepinsky, et al., The morphogen sonic hedgehog is an indirect angiogenic agent upregulating two families of angiogenic growth factors, *Nat. Med.* 7 (6) (2001 Jun) 706–711.
- [8] K.F. Kusano, R. Pola, T. Murayama, C. Curry, A. Kawamoto, A. Iwakura, et al., Sonic hedgehog myocardial gene therapy: tissue repair through transient reconstitution of embryonic signaling, *Nat. Med.* 11 (11) (2005 Nov) 1197–1204.
- [9] R. Pola, L.E. Ling, T.R. Aprahamian, E. Barban, M. Bosch-Marce, C. Curry, et al., Postnatal recapitulation of embryonic hedgehog pathway in response to skeletal muscle ischemia, *Circulation* 108 (4) (2003 Jul 29) 479–485.
- [10] P.M. Lewis, M.P. Dunn, J.A. McMahon, M. Logan, J.F. Martin, B. St-Jacques, et al., Cholesterol modification of sonic hedgehog is required for long-range signaling activity and effective modulation of signaling by Ptc1, *Cell* 105 (5) (2001 Jun 1) 599–612.
- [11] N.S. Chari, T.J. McDonnell, The sonic hedgehog signaling network in development and neoplasia, *Adv. Anat. Pathol.* 14 (5) (2007 Sep) 344–352.
- [12] M. Varjosalo, J. Taipale, Hedgehog signaling, *J. Cell Sci.* 120 (Pt 1) (2007 Jan 1) 3–6.
- [13] Q. Xiao, N. Hou, Y.P. Wang, L.S. He, Y.H. He, G.P. Zhang, et al., Impaired sonic hedgehog pathway contributes to cardiac dysfunction in type 1 diabetic mice with myocardial infarction, *Cardiovasc. Res.* 95 (4) (2012 Sep 1) 507–516.
- [14] J. Roncalli, M.A. Renault, J. Tongers, S. Misener, T. Thorne, C. Kamide, et al., Sonic hedgehog-induced functional recovery after myocardial infarction is enhanced by AMD3100-mediated progenitor-cell mobilization, *J. Am. Coll. Cardiol.* 57 (24) (2011 Jun 14) 2444–2452.
- [15] K. Ueda, H. Takano, Y. Niitsuma, H. Hasegawa, R. Uchiyama, T. Oka, et al., Sonic hedgehog is a critical mediator of erythropoietin-induced cardiac protection in mice, *J. Clin. Invest.* 120 (6) (2010 Jun) 2016–2029.
- [16] K.J. Lavine, A. Kovacs, D.M. Ornitz, Hedgehog signaling is critical for maintenance of the adult coronary vasculature in mice, *J. Clin. Invest.* 118 (7) (2008 Jul) 2404–2414.
- [17] N. Mizushima, T. Yoshimori, B. Levine, Methods in mammalian autophagy research, *Cell* 140 (3) (2010 Feb 5) 313–326.
- [18] C. Behrends, M.E. Sowa, S.P. Gygi, J.W. Harper, Network organization of the human autophagy system, *Nature* 466 (7302) (2010 Jul 1) 68–76.
- [19] D.J. Klionsky, F.C. Abdalla, H. Abeliovich, R.T. Abraham, A. Acevedo-Arozena, K. Adeli, et al., Guidelines for the use and interpretation of assays for monitoring autophagy, *Autophagy* 8 (4) (2012 Apr) 445–544.
- [20] K. Przyklenk, V.V. Undyala, J. Wider, J.A. Sala-Mercado, R.A. Gottlieb, R.M. Mentzer Jr., Acute induction of autophagy as a novel strategy for cardioprotection: getting to the heart of the matter, *Autophagy* 7 (4) (2011 Apr) 432–433.
- [21] H. Takagi, Y. Matsui, J. Sadoshima, The role of autophagy in mediating cell survival and death during ischemia and reperfusion in the heart, *Antioxidants Redox Signal.* 9 (9) (2007 Sep) 1373–1381.
- [22] S.M. Samuel, M. Thirunavukkarasu, S.V. Penumathsa, S. Koneru, L. Zhan, G. Maulik, et al., Thiorodexin-1 gene therapy enhances angiogenic signaling and reduces ventricular remodeling in infarcted myocardium of diabetic rats, *Circulation* 121 (10) (2010 Mar 16) 1244–1255.
- [23] J.-D. Luo, T.-P. Hu, L. Wang, M.-S. Chen, S.-M. Liu, A.F. Chen, Sonic hedgehog improves delayed wound healing via enhancing cutaneous nitric oxide function in diabetes, *Am. J. Physiol. Endocrinol. Metab.* 297 (2) (2009) E525–E531.
- [24] N. Mizushima, T. Yoshimori, How to interpret LC3 immunoblotting, *Autophagy* 3 (6) (2007 Nov–Dec) 542–545.
- [25] J.M. Vicencio, L. Galluzzi, N. Tajeddine, C. Ortiz, A. Criollo, E. Tasdemir, et al., Senescence, apoptosis or autophagy? when a damaged cell must decide its path—a mini-review, *Gerontology* 54 (2) (2008) 92–99.
- [26] M.C. Maiuri, E. Zalckvar, A. Kimchi, K. Kroemer, Self-eating and self-killing: crosstalk between autophagy and apoptosis, *Nat. Rev. Mol. Cell Biol.* 8 (9) (2007 Sep) 741–752.
- [27] B. Levine, J. Yuan, Autophagy in cell death: an innocent convict? *J. Clin. Invest.* 115 (10) (2005 Oct) 2679–2688.
- [28] J. Kim, M. Kundu, B. Viollet, K.L. Guan, AMPK and mTOR regulate autophagy through direct phosphorylation of Ulk1, *Nat. Cell Biol.* 13 (2) (2011 Feb) 132–141.
- [29] K. Inoki, J. Kim, K.L. Guan, AMPK and mTOR in cellular energy homeostasis and drug targets, *Annu. Rev. Pharmacol. Toxicol.* 52 (2012) 381–400.
- [30] D.F. Egan, D.B. Shackelford, M.M. Mihaylova, S. Gelino, R.A. Kohnz, W. Mair, et al., Phosphorylation of ULK1 (hATG1) by AMP-activated protein kinase connects energy sensing to mitophagy, *Science* 331 (6016) (2011 Jan 28) 456–461.
- [31] M.M. Mihaylova, R.J. Shaw, The AMPK signalling pathway coordinates cell growth, autophagy and metabolism, *Nat. Cell Biol.* 13 (9) (2011 Sep) 1016–1023.
- [32] D. Egan, J. Kim, R.J. Shaw, K.L. Guan, The autophagy initiating kinase ULK1 is regulated via opposing phosphorylation by AMPK and mTOR, *Autophagy* 7 (6) (2011 Jun) 643–644.
- [33] D.G. Hardie, F.A. Ross, S.A. Hawley, AMP-activated protein kinase: a target for drugs both ancient and modern, *Chem. Biol.* 19 (10) (2012 Oct 26) 1222–1236.
- [34] M.B. Chen, W.X. Shen, Y. Yang, X.Y. Wu, J.H. Gu, P.H. Lu, Activation of AMP-activated protein kinase is involved in vincristine-induced cell apoptosis in B16 melanoma cell, *J. Cell Physiol.* 226 (7) (2011 Jul) 1915–1925.
- [35] M.R. Kang, S.K. Park, C.W. Lee, I.J. Cho, Y.N. Jo, J.W. Yang, et al., Widdrol induces apoptosis via activation of AMP-activated protein kinase in colon cancer cells, *Oncol. Rep.* 27 (5) (2012 May) 1407–1412.
- [36] Q.Y. Zheng, F.S. Jin, C. Yao, T. Zhang, G.H. Zhang, X. Ai, Ursolic acid-induced AMP-activated protein kinase (AMPK) activation contributes to growth inhibition and apoptosis in human bladder cancer T24 cells, *Biochem. Biophys. Res. Commun.* 419 (4) (2012 Mar 23) 741–747.
- [37] P. Narbonne, R. Roy, Caenorhabditis elegans dauers need LKB1/AMPK to ration lipid reserves and ensure long-term survival, *Nature* 457 (7226) (2009 Jan 8) 210–214.
- [38] S.M. Jeon, N.S. Chandel, N. Hay, AMPK regulates NADPH homeostasis to promote tumour cell survival during energy stress, *Nature* 485 (7400) (2012 May 31) 661–665.